

ALOS-PALSAR Image Simulation in Various Polarization Bases

Yoshio Yamaguchi, Koji Kimura, Sohei Kakizaki, and Hiroyoshi Yamada

Department of Information Engineering, Niigata University

Ikarashi 2-8050, Niigata 950-2181, Japan

Abstract - The ALOS-PALSAR is the first L-band space-borne SAR in the world equipped with fully polarimetric data take function. For the data utilization purpose, the authors have examined the polarimetric performance (scattering matrix and resultant images) over Toyano Area, Niigata City, Japan, using the airborne Pi-SAR radar. Since the resolution will be 20 m by 20 m on the ground surface by PALSAR, the Pi-SAR data (3 m by 3 m) are ensemble to be equivalent size for ALOS-PALSAR image simulation. Then the polarimetric characteristics of terrain including paddy-fields, grass-fields, residential area, etc., were examined to show the difference in the RL basis and coherency vector, three-component scattering model, and polarimetric entropy.

I. INTRODUCTION

ALOS-PALSAR is the first spaceborne L-band polarimetric SAR to be launched in 2004. The attracting feature is its polarimetric mode as listed in Table I.

Frequency	1270 MHz
Bandwidth	14 MHz
Incidence angle	8-30 degrees
Range resolution	24-89 m
Swath	20-65 km

Fortunately, a Polarimetric and Interferometric Synthetic Aperture Radar (named Pi-SAR), developed by Communication Research Laboratory (CRL) and NASDA, Japan, has provided high resolution polarimetric data sets in these years. The authors used the Pi-SAR data sets for simulations of PALSAR performance. The L-band polarimetric data contain high resolution scattering matrices of 3 m by 3 m both in the range and azimuth direction on the ground. These data can be ensemble to be of any multiple resolution size for polarimetric scattering characteristics investigation. In the following, some polarization images, correlation coefficients for several targets, and classification results of land cover are shown.

II. POLARIZATION IMAGES

For the simulation, the L-band Pi-SAR data of Toyano Area, acquired on Oct. 2, 2000, are used. The features of Pi-SAR systems for the L-band polarimetric data sets are listed in Table II. At first, we made polarimetric calibration [1] to Pi-SAR data. Then we adjusted the resolution (3 m) of Pi-SAR to become that (20 m) of ALOS-PALSAR. If

scattering matrix data are provided, it is possible to apply various polarimetric analyses. For example, polarimetric SAR images can be constructed in various polarization bases such as circular Right-Left hand basis, coherency vector component basis, and three-component scattering model [2]-[5]. Several polarization images among them are shown in Fig. 1. The area is rich in specific targets such as water region (lake and river), soil (paddy and grass field), residential houses, soccer stadium, park, highway junction, etc.

Table II L-BAND Pi-SAR CHARACTERISTICS

Data-take	14 October, 1999
Frequency	1.27 GHz
Polarization	HH, HV, VH, VV
Incidence angle	46.99-55.79 degrees
Resolution	3.0 m az. X 3.0 m slt-rng.
Pixel Spacing	2.5 m az. X 2.4 m slt-rng.

III. CLASSIFICATION

Land classification was carried out by maximum-likelihood method using polarimetric indices. The feature vector component are :

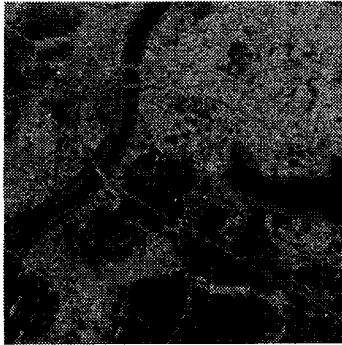
- scattering matrix components RR, RL, LL in the circular polarization basis,
- coherency vector component HH+VV, HH-VV, 2HV and polarimetric entropy and averaged alpha angle [4],
- three- scattering component P_s, P_d, P_v [5],

The classification results are shown in Table III. For classification, three main classes of land cover, i.e., water region, soil, and residential area, are chosen in Fig. 2. It is seen from Table III that coherency vector and three-component scattering model shows good performance. Detailed results on finding effective polarimetric indices for target classification will be shown in the presentation.

IV. RESOLUTION CHANGES

It is interesting to see how the polarimetric characteristics change with resolution. Since the Pi-SAR resolution is fine, we tried intentionally to change the resolution cell by averaging the pixel and examined the correlation coefficients in the RR to LL, and in the HH+VV to HH-VV. The correlations in the specific rectangular boxes (areas A-F) in Fig. 2 are shown in Fig. 3 as a function of resolution size.

Area A and B Residential area, with a lot of houses, heterogeneous



RR



HH+VV



P_s



RL



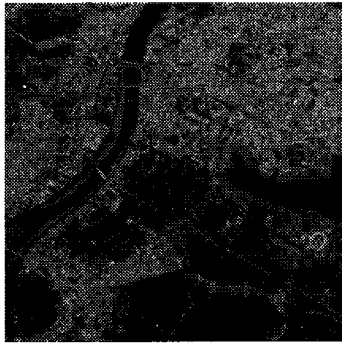
HH-VV



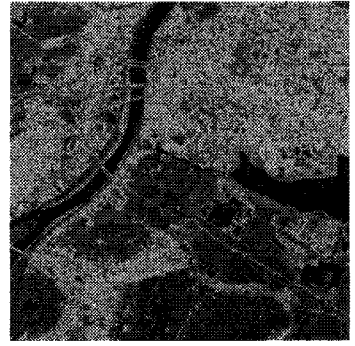
P_d



LL



2HV



P_v

(a) RR, RL, LL

(b) HH+VV, HH-VV, 2HV

(c) P_s , P_d , P_v

Fig. 1. Polarization images.

TABLE III CLASSIFICATION ACCURACY TABLES [%].

(a) RR, RL, LL			
	Water	Soil	Residential
Water	94.66	4.62	0.72
Soil	25.55	65.58	8.87
Residential	0.16	9.64	90.20
Total = 85.75 %			
(b) HH+VV, HH-VV, 2HV			
	Water	Soil	Residential
Water	95.82	3.46	0.72
Soil	10.61	81.72	7.67
Residential	0.03	7.17	92.80
Total = 90.86 %			
(c) P_s, P_d, P_v			
	Water	Soil	Residential
Water	95.60	3.46	0.94
Soil	10.27	80.97	8.76
Residential	0.03	6.64	93.33
Total = 91.10 %			
(d) Polarimetric entropy H and $\bar{\alpha}$			
	Water	Soil	Residential
Water	80.74	14.43	4.83
Soil	24.04	50.12	25.84
Residential	9.71	40.18	50.11
Total = 52.25 %			

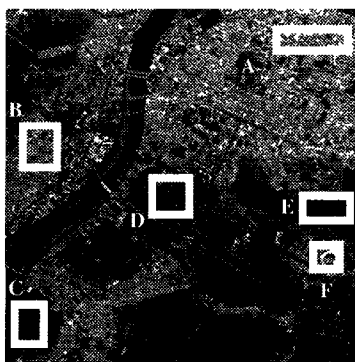


Fig. 2. Specific targets for analysis.

- Area C and D** Soil, with surface roughness; distributed and homogeneous
- Area E** Lake, distributed and homogeneous
- Area F** Soccer stadium

Since the value of correlation does not change in the regions larger than 20 m, the PALSAR polarimetric images may be suitable for land cover classifications.

V. CONCLUDING REMARKS

Pi-SAR scattering matrix data are used to simulate ALOS-PALSAR image analysis. Although the incidence angle is different, the resolution of 20 m of PALSAR and its scattering

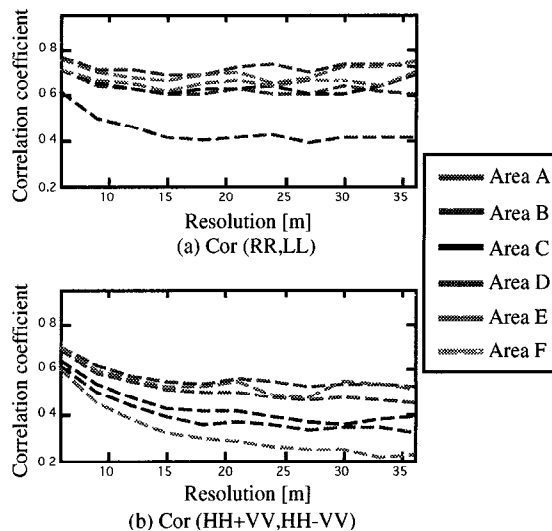


Fig. 3. Correlation coefficients as a function of resolution size.

matrix will contribute land cover classification effectively.

ACKNOWLEDGMENT

The authors are grateful to Pi-SAR data provided by CRL/NASDA. This work in part was carried out by Grant-in-Aid for Scientific Research, the Ministry of Education, Japan.

REFERENCES

- [1] S. Quegan, "A Unified Algorithm for Phase and Cross-Talk Calibration of Polarimetric Data-Theory and Observation," *IEEE Trans. Geosci. Remote Sensing*, vol. 32, no. 1, pp. 89-99, Jan. 1994.
- [2] C. T. Schneider, "Polarimetric analysis of RAMSES SAR images," *Proc. of 4th international workshop on radar polarimetry*, pp. 366-375, July 1998.
- [3] E. Hanle, "New Contemplations on Polarimetric Decomposition Based on Expected Target Orientation," *Proc. of 4th international workshop on radar polarimetry*, pp. 67-76, July 1998.
- [4] S. R. Cloude, and E. Pottier, "A Review of Target Decomposition Theorems in Radar Polarimetry," *IEEE Trans. Geosci. Remote Sensing*, vol. 34, no. 2, pp. 498-518, Mar. 1996.
- [5] A. Freeman, and S. Durden, "A Three-Component Scattering Model for Polarimetric SAR Data," *IEEE Trans. Geosci. Remote Sensing*, vol. 36, no. 3, pp.963-973, May 1998.